1 Introduction

The development of modern internal combustion engines faces several key challenges such as strict emission regulations or further efficiency improvements in addition to meeting the customer demand and the targets regarding development cost and time. As a result of these objectives, complex questions and conflicts arise which have to be appropriately resolved during the design process. In the past, this process was almost exclusively driven by experiments. Due to the exponential increase in computational power, Computational Fluid Dynamics (CFD) took over this leading role, particularly in early development stages. Numerical simulation is now a fast and inexpensive method to study and optimize the design of an engine in a coherent way without having to manufacture costly prototypes. Moreover, additional insight into physical phenomena, which are not or hardly accessible by experiments, can be obtained by simulation contributing to the understanding of the physics within a combustion engine.

To simulate the combustion process in a modern spark-ignition (SI) engine, the physics of chemistry, thermodynamics, fluid mechanics and turbulence as well as their microscopic interaction have to be appropriately reproduced. Although each of these processes is largely understood on its own, their prediction via Direct Numerical Simulation (DNS) is not yet feasible for large-scale industrial applications such as spark-ignition engines and it is questionable if this will ever be a viable option. Reynolds-Averaged Navier-Stokes (RANS) methods are thus expected to remain the backbone of industrial CFD simulations due to their efficiency. The RANS approach only resolves the flow on a macroscopic level and thus requires physical sub-models to describe the microscopic interaction of turbulence and combustion on a macroscopic scale. The vast majority of flows in engineering applications such as IC engines is bounded by walls rendering the treatment of the wall a key factor determining the overall accuracy of the simulation. While an abundant literature on non-reacting flows can be found, few literature on reactive wall-bounded flows is available. Almost all combustion models lack a profound physical description of the flame-wall interaction process and use intuitive approaches to overcome their basic flaws near the wall. Consequently, the predictive capabilities of combustion models are still limited.

The scope of this problem is enhanced by the fact that every SI engine is subjected to flame-wall interactions. The interaction of a premixed flame with the combustion chamber walls substantially influences the wall heat losses, engine-out emissions and the combustion efficiency. Despite its significance, little is known to date on its nature and experimental data is scarce. The main objectives of this thesis are thus to clarify the phenomenology of flame-wall interactions in SI engines and to subsequently develop a comprehensive combustion modelling approach on this basis.

As a starting point, a coherent picture of premixed flame-wall interactions is established based on the available literature. Laminar and turbulent flame-wall interactions as well as near-wall turbulence are discussed separately to discern the individual contributions of wall heat loss, chemical reactions and turbulence. Based on this a priori analysis, it is suggested that the interaction of a premixed flame with the walls of a SI engine is similar to the one observed for laminar premixed flames.

To prove or disprove this hypothesis, an extensive analysis of flame-wall interactions in a modern direct-injection SI engine is carried out. For this purpose, a highly-resolved measurement of the wall heat flux at the combustion chamber walls is combined with a comprehensive simulative workflow. Several operating points are examined to study the influence of speed, load, equivalence ratio and charge motion on the quenching process. The simulative workflow consists of several 3D-CFD, 3D-FE and 1D simulations in order to accurately predict the flow state as well as the laminar flame properties near the combustion chamber walls. Using this information, the cycle-resolved wall heat fluxes are analysed and the characteristics of the quenching process such as quenching distances are determined. The results are examined in detail and provide new insights into the physics of the quenching process in a SI engine.

Finally, a modelling approach that accounts for the previously identified main effects of flame-wall interactions, flame quenching and near-wall turbulence, is proposed. The aim is to correctly describe the near-wall behaviour of turbulent premixed flames based on a comprehensive theoretical approach. For this purpose, the framework of the *G*-equation combustion model, which has proven to successfully predict combustion processes in SI engines, is used. A virtue of the *G*-equation, which is also exploited in this work, is that standard modelling techniques of non-reacting turbulent flows can be applied. Following classic combustion modelling guidelines, the structure of a laminar quenched flame and a kinematic equation describing its behaviour is derived. The approach is transferred to turbulent flames by determining the probability of finding quenched flamelets within a turbulent flame brush and its impact on the turbulent burning velocity. The *G*-equation combustion model is subsequently extended to also describe partially or fully quenched turbulent flames. The impact of near-wall turbulence and flame development on the turbulent burning velocity as well as on the model closures is discussed and appropriate relations are provided. The presented approaches can also be applied to other combustion models, in particular to those that are based on the turbulent burning velocity. The resulting *G*-equation Flame-Wall Interaction (GFWI) model is subsequently analysed in an a priori fashion and tested against DNS data. Furthermore, it is applied to simulate combustion in SI engines and the impact of flame-wall interaction on the combustion process is studied. Finally, the experimental and simulative results are combined to draw a comprehensive phenomenological picture of flame-wall interactions in SI engines.

This work is divided into seven chapters. In chapter 2, the fundamentals of reactive flows, turbulence and premixed flames are briefly introduced. After presenting the governing equations for chemically reacting flows, the phenomenon of turbulence and its characteristic scales is discussed and the conservation equations are given in their reynolds-averaged form. The closure of the RANS equations is shortly addressed before the fundamentals of premixed combustion are discussed. Particular emphasis is laid on the description of the physics of laminar and turbulent premixed flames. The chapter is concluded by a short overview of the common modelling approaches for turbulent premixed flames.

A detailed analysis of flame-wall interactions based on the available literature is given in chapter 3. At first, laminar flame-wall interactions are examined in detail by focussing on the chemical reactions and the characteristics of the quenching process such as the wall heat flux. The basics of wall-bounded turbulent flows are introduced and turbulent flame-wall interactions are discussed on this basis. Finally, an a priori analysis of flame-wall interactions in SI engines as well as a brief literature review on flame-wall interaction models is presented.

Chapter 4 is devoted to the analysis of flame-wall interactions by a combined experimental and simulative approach. First, the experimental setup and procedure is presented before the measured wall heat fluxes are analysed on a phenomenological basis. The evaluation of the quenching process and the required simulative workflow are described thereafter. Finally, the results of the combined analysis are discussed in detail.

In Chapter 5, the modelling approach is presented. First, the original G-equation model is introduced before the modelling of flame quenching is discussed in detail. Based on the results, a consistent level-set approach for turbulent quenched and unquenched flames is introduced and complemented by modelling closures that take near-wall turbulence and flame development into account. The most important modelling assumptions of the GFWI model are reviewed and the model performance is analysed using a turbulent channel flow and a simple SI engine test case.

The application of the GFWI model to simulate combustion in a direct-injection SI engine is shown in chapter 6. The combustion simulation results are analysed and a summary of the phenomenology of flame-wall interactions in SI engines is provided.

Finally, the main findings of this thesis and possible areas for future work are summarized in chapter 7.

2 Fundamentals of reactive flows, turbulence and premixed flames

The vast majority of flows and combustion processes encountered in engineering problems are turbulent due to their ability to mix transported quantities much more effectively than molecular diffusion processes. However, turbulence is one of the most complex phenomenons encountered in classical physics due to its seemingly erratic and chaotical behaviour. As a consequence, many approaches describing turbulence based on different assumptions have been developed. For this reason, modelling requires an in-depth knowledge of the underlying concepts as well as the related equations. A comprehensive introduction in turbulent flows is out of the scope of this work and can be found in relevant textbooks, e.g., Pope [154]. This chapter is dedicated to introduce the physics of turbulent reactive flows in the context of the Reynolds-Averaged Navier Stokes (RANS) equations with a focus on turbulent premixed flames.

For this purpose, the instantaneous conservation equations for reacting flows are introduced in combination with the necessary constitutive and state relations in section 2.1. Section 2.2 contains a brief introduction to the nature of turbulence and its characteristic scales as well as a presentation of the Reynolds-Averaged Navier Stokes equations. Moreover, classical turbulence closures based on the turbulent-viscosity and gradient-diffusion hypotheses are shown. This chapter is concluded with an introduction to premixed combustion in section 2.3. Special emphasis is laid on the physics of laminar as well as turbulent premixed flames and the related physical concepts. Finally, the most important models for turbulent premixed combustion modelling are presented.

2.1 Governing Equations

The governing equations for turbulent reacting flows are commonly expressed by transport equations for continuity, momentum, species mass fractions and energy as well as constitutive relations for atomistic processes (e.g., diffusion, equation of state). Various forms of these equations, especially of the energy equation, can be found in literature. For a detailed discussion, the reader is referred to the books of Williams [212] and Poinsot and Veynante [150]. The following part focuses on the relations commonly used for turbulent combustion modelling and simulation.

2.1.1 Conservation equations

The instantaneous governing equations of a compressible flow are given by the transport equations for density, momentum, species mass fractions and enthalpy. In their conservative form, these equations read

$$\frac{\partial \rho}{\partial t} + \nabla \cdot (\rho \mathbf{v}) = 0 \tag{2.1}$$

$$\frac{\partial \rho \mathbf{v}}{\partial t} + \nabla \cdot (\rho \mathbf{v}\mathbf{v}) + \nabla p - \nabla \cdot \boldsymbol{\tau} = 0 \tag{2.2}$$

$$\frac{\partial \rho h}{\partial t} + \nabla \cdot (\rho \mathbf{v} h) - \frac{\partial p}{\partial t} - \mathbf{v} \cdot \nabla p + \nabla \cdot \mathbf{q} - \boldsymbol{\tau} : \nabla \mathbf{v} - \dot{Q} = 0 \tag{2.3}$$

$$\frac{\partial \rho Y_\alpha}{\partial t} + \nabla \cdot (\rho \mathbf{v} Y_\alpha) + \nabla \cdot \mathbf{j}_\alpha - \dot{\omega}_\alpha = 0 \tag{2.4}$$

when volume forces are neglected. In the above equations, ρ denotes the density, $\mathbf{v}$ the velocity vector, p the pressure, $\boldsymbol{\tau}$ the viscous stress tensor, h the enthalpy, $\mathbf{q}$ the heat flux vector, $\dot{Q}$ a heat source term, Y_α the mass fraction of species α, $\mathbf{j}_\alpha$ its diffusive flux vector and $\dot{\omega}_\alpha$ its source term. The equations (2.1)-(2.4) are solved for $(\rho, \rho\mathbf{v}, \rho h, \rho\mathbf{Y})$.

As already indicated, there are several different possibilities to formulate the energy equation (Eq. (2.3)). A comprehensive overview can be found in the textbook by Poinsot and Veynante [150]. In the present work, the transport equation for the enthalpy h is utilized. Therein, h is the sum of the specific enthalpy h_α of each species α defined by

$$h_\alpha = h^0_{f,\alpha} + \int_{T_{ref}}^{T} c_{p,\alpha} dT. \tag{2.5}$$

In this equation, $h^0_{f,\alpha}$ denotes the standard enthalpy of formation at a specific reference temperature T_{ref} (usually 298.15K) and $c_{p,\alpha}$ the specific heat capacity at constant pressure. Hence, h can be written as

$$h = \sum_{i=1}^{N} h_\alpha Y_\alpha = \int_{T_{ref}}^{T} c_p dT + \sum_{\alpha=1}^{N} h^0_{f,\alpha} Y_\alpha \quad \text{where} \quad c_p = \sum_{i=1}^{N} c_{p,\alpha} Y_\alpha \tag{2.6}$$

is the specific heat capacity at constant pressure of the mixture. Since h is composed of the sensible and chemical enthalpy, there is no source term due to reaction in the energy equation (Eq. (2.3)).

2.1.2 Constitutive and state equations, transport properties

To complete this set of equations, constitutive and state equations as well as relations for the transport properties are required. These relations introduce atomistic processes and relate them to the continuous quantities $(\rho, \mathbf{v}, h, \mathbf{Y})$. Commonly, turbulent reacting flows are treated as a Newtonian fluid and as an ideal gas. Hence, the thermal equation of state relating the density ρ, the pressure p and the temperature T is given by

$$p = \rho R T \tag{2.7}$$

where R is the gas constant. It can be calculated for a given composition by utilizing the mean molar mass M of the mixture or the molar masses M_α in combination with the species mass fractions Y_α:

$$R = \frac{\mathcal{R}}{M} = \mathcal{R} \sum_{\alpha=1}^{N} \frac{Y_\alpha}{M_\alpha}. \tag{2.8}$$

The universal gas constant is represented by $\mathcal{R}$. Using Stokes' hypothesis, the constitutive relation for the viscous stress tensor $\boldsymbol{\tau}$ of a Newtonian fluid is defined by

$$\boldsymbol{\tau} = \mu \left[(\nabla \mathbf{v}) + (\nabla \mathbf{v})^T \right] - \frac{2}{3} \mu \left(\nabla \cdot \mathbf{v} \right) \mathbf{I}. \tag{2.9}$$

Here, $\mathbf{I}$ denotes the unit tensor and μ the dynamic viscosity of the mixture.
In addition to these relations, the transport processes defining the flux vectors $\mathbf{j}_\alpha$ and $\mathbf{q}$ have to be appropriately determined. According to Hirschfelder et al. [91], the heat flux vector $\mathbf{q}$ consists of three individual contributions from different modes of heat transfer. These are heat conduction, heat diffusion by species diffusion and thermal diffusion (Dufour effect). The latter is negligible for almost any combustion process (Gerlinger [76]). Using the Fourier's law for heat conduction, the heat flux vector $\mathbf{q}$ reads

$$\mathbf{q} = -\lambda \nabla T + \sum_{i=1} h_\alpha \, \mathbf{j}_\alpha \tag{2.10}$$

where λ represents the thermal conductivity. Similar to the heat flux vector $\mathbf{q}$, the diffusive flux vector $\mathbf{j}_\alpha$ can also be decomposed in different parts, namely diffusion by concentration gradients (Fickian diffusion), thermal diffusion (Soret effect) and pressure diffusion. The latter does have a negligible role compared to the former ones, since the spatial pressure gradients are usually small. The Soret-effect becomes important for light species or large temperature gradients (e.g., for laminar hydrogen-air flames) and is negligible for turbulent flames (cf. Gerlinger [76]). As a result, the diffusive flux is commonly modelled by the binary flux approximation (Peters [142]):

$$\mathbf{j}_\alpha = -\rho D_\alpha \nabla Y_\alpha = -\frac{\mu}{Sc_\alpha} \nabla Y_\alpha \qquad \text{with} \qquad Sc_\alpha = \frac{\nu}{D_\alpha}. \tag{2.11}$$

Therein, D_α denotes the binary diffusion coefficient of species α with respect to an abundant species like N_2. The Schmidt number Sc_α compares the momentum and molecular diffusion of species α. However, this approximation violates the mass conservation in a multicomponent system for unequal diffusion coefficients D_α. For simplicity, it is thus assumed that all mass diffusivities D_α are equal and proportional to the thermal diffusivity $D = \lambda / \rho c_p$ yielding constant Lewis numbers,

$$Le_\alpha = \frac{\lambda}{\rho c_p D_\alpha} = \frac{D}{D_\alpha}. \tag{2.12}$$

These relations can be used to simplify the heat flux vector $\mathbf{q}$. By spatially differentiating the definition of the enthalpy h and inserting the result in Eq. (2.10), one arrives at

$$\mathbf{q} = -\frac{\mu}{Pr} \nabla h + \sum_{\alpha=1} h_\alpha \left(\frac{\mu}{Pr} - \frac{\mu}{Sc_\alpha} \right) \nabla Y_\alpha \tag{2.13}$$

where the Prandtl number

$$Pr = \frac{\mu c_p}{\lambda} \tag{2.14}$$

was introduced (Gerlinger [76]). A common assumption for turbulent flows is a unity Lewis number, i.e., $Le_\alpha = Sc_\alpha/Pr = 1$. Hence, Eq. (2.13) can be further simplified and the relations for the diffusive and heat flux read

$$\mathbf{j}_\alpha = -\frac{\mu}{Sc_\alpha}\nabla Y_\alpha\,, \tag{2.15}$$

$$\mathbf{q} = -\frac{\mu}{Pr}\nabla h\,. \tag{2.16}$$

A more detailed discussion of transport processes can be found in Bird et al. [20] and Hirschfelder et al. [91].

The last remaining term which has to be suitably determined is the chemical source term. The chemistry is commonly described by a collection of elementary reactions comprising multiple transition states and intermediate species. Due to the complexity and nonlinearity of combustion, considerable effort was put into the research and development of suitable reaction mechanisms (Westbrook et al. [209]). For example, reaction mechanisms which accurately describe the behaviour of long-chain hydrocarbons can consist of several hundred species and thousands of reactions (cf. Cai et al. [32]). The general notation of a reaction mechanism comprising M (single step) reactions and N species reads

$$\sum_{\alpha=1}^{N} \upsilon'_{\alpha r}\mathsf{M}_\alpha \underset{k_{br}}{\overset{k_{fr}}{\rightleftharpoons}} \sum_{\alpha=1}^{N} \upsilon''_{\alpha r}\mathsf{M}_\alpha \qquad \text{for} \qquad r = 1, \ldots, M, \tag{2.17}$$

where M_α is the chemical symbol for species α and $\upsilon'_{\alpha r}$ and $\upsilon''_{\alpha r}$ are the stoichiometric coefficients of reaction r in forward and backward direction, respectively. Correspondingly, k_{fr} and k_{br} are the reaction rate coefficients of the forward respectively backward reaction. For each reaction, a reaction rate $\dot{w}_r$ can be defined

$$\dot{w}_r = k_{fr}\prod_{\beta=1}^{N}\left(\frac{\rho Y_\beta}{M_\beta}\right)^{\upsilon'_{\beta r}} - k_{br}\prod_{\beta=1}^{N}\left(\frac{\rho Y_\beta}{M_\beta}\right)^{\upsilon''_{\beta r}} \tag{2.18}$$

The reaction rate coefficients k_{fr} and k_{br} comprise statistical information about the rate of collisions, the fraction of collisions resulting in a reaction and a factor taking the shape of the molecules into account. They are commonly modelled by the empirical Arrhenius equation

$$k_r(T) = A_r T^{\beta_r}\exp\left(-\frac{E_r}{\mathcal{R}T}\right) \tag{2.19}$$

where A_r is a frequency factor, β_r the temperature exponent and E_r the activation energy. The main challenge of chemical kinetics lies in providing these values as well as determining the most important reactions and species to keep the reaction mechanism as lean as possible (Warnatz et al. [203]). The reaction rate $\dot{\omega}_\alpha$ of each species α can then be determined by addition of all relevant reaction rates $\dot{w}_r$

$$\dot{\omega}_\alpha = M_\alpha \sum_{r=1}^{M}\left(\upsilon''_{\alpha r} - \upsilon'_{\alpha r}\right)\dot{w}_r\,. \tag{2.20}$$

2.2 Turbulence

Turbulence is a three-dimensional and unsteady phenomenon where the fluid velocity varies seemingly chaotic in space and time. A common feature of all turbulent flows is the existence of a multitude of eddies of different sizes. These eddies enhance diffusion and mixing processes which are essential for a large range of applications including internal combustion engines. For a comprehensive introduction and discussion of turbulent flows and its manifold aspects, the reader is referred to the textbook of Pope [154]. The following discussion focuses on homogeneous, isotropic turbulence. In general, turbulence in near-wall flows is anisotropic. This circumstance plays an important role during flame-wall interactions and is discussed separately in chapter 3.

2.2.1 Scales of turbulent motion

Flows become turbulent when the convective forces are large compared to the viscous forces. In this case, small disturbances (e.g., the roughness of a wall) can lead to a transition from a laminar to a turbulent flow. Unstable eddies are formed which continuously break-up and induce smaller eddies. This process continues until the kinetic energy of the eddies is finally dissipated at the turbulent dissipation rate ε due to the viscous forces. The idea of a steady transfer of kinetic energy from large to small scales until its viscous dissipation was first proposed by Kolmogorov [103] and is called the eddy cascade hypothesis.

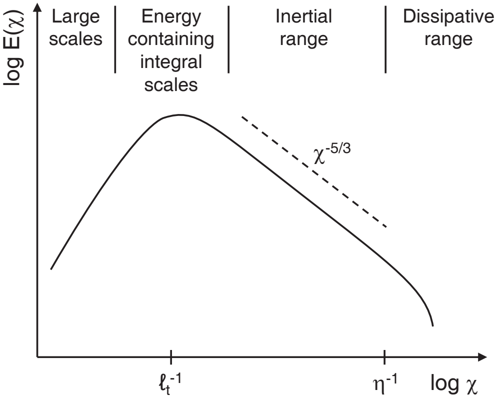

Figure 2.1: Energy spectrum of homogeneous, isotropic turbulence (adapted from Peters [142]).

The resulting energy spectrum $E(\chi)$ of homogeneous, isotropic turbulence is shown in Fig. 2.1. Small eddies are associated to large spatial wave numbers χ and vice versa. The turbulent kinetic energy k of eddy motion defined by the trace of the Reynolds stress tensor can be related to the energy spectrum as follows

$$k = \frac{1}{2}\overline{\mathbf{v}' \cdot \mathbf{v}'} = \int_0^\infty E(\chi) d\chi, \tag{2.21}$$

where $\mathbf{v}'$ is the fluctuation of the velocity. The eddy motion in a turbulent flow can be characterized by distinctive length scales and turnover times. Based upon the similarity analysis by Kolmogorov [103], the turbulent energy spectrum is usually subdivided in four different ranges. The first range depends on the boundary conditions of the flow and is thus not universal. It comprises the largest eddies which are of the size of the mean flow scales. The second range contains the integral scale eddies which comprise most of the energy of the turbulent flow. Moreover, the production of turbulence by mean velocity gradients also peaks in this region. There are various definitions and approximations of the integral length scale, however, all are proportional to

$$\ell_t = \frac{k^{3/2}}{\varepsilon}. \tag{2.22}$$

Bray [27] defined the turbulent length scale as

$$l_t = a_1 \frac{v'^3}{\varepsilon} \qquad \text{with} \qquad a_1 = 0.37. \tag{2.23}$$

Another definition originates from the law of the wall in combination with k-ε-turbulence models. By assuming a local balance between the production and dissipation of turbulent kinetic energy in the logarithmic law region, the mixing length l_m is related to k and ε by

$$l_m = \kappa y = c_\mu^{3/4} \frac{k^{3/2}}{\varepsilon} \qquad \text{with} \qquad c_\mu = 0.09. \tag{2.24}$$

Here, $\kappa \approx 0.41$ denotes the von-Kármán constant and y the wall distance. The expressions l_t and l_m for the integral length scale differ in magnitude by around 20% (Ewald [66]). An important quantity for combustion modelling is the turnover velocity of integral size eddies v' defined as

$$v' = \sqrt{\frac{2}{3}k}, \tag{2.25}$$

often referred to as turbulence intensity denoted by either u' or v'. The turnover time of the energy containing eddies is called the integral time scale and is defined as

$$\tau = \frac{k}{\varepsilon}. \tag{2.26}$$

The third range, called inertial range, is characterized by a steady energy transfer towards the smaller scales. Therein, production and dissipation of turbulence is negligible. Using dimensional analysis, it can be shown that the energy spectrum obeys the scaling law

$$E(\chi) \sim \varepsilon^{2/3} \chi^{-5/3}. \tag{2.27}$$